Laser and Particle Beams (2003), *21*, 609–614. Printed in the USA.

DOI: 10.1017/S0263034603214208

Numerical analysis of a multilayered cylindrical target compression driven by a rotating intense heavy ion beam

M. TEMPORAL,[1] A.R. PIRIZ,[1] N. GRANDJOUAN,[2] N.A. TAHIR,[3] AND D.H.H. HOFFMANN[4,5]

[1]Universidad de Castilla-La Mancha, Ciudad Real, Spain
[2]LULI, UMR 7605, École Polytechnique, CNRS, CEA, Université Paris VI, Palaiseau, France
[3]Institut für Theoretische Physik, Universität Frankfurt, Frankfurt, Germany
[4]Institut für Kernphysik, Technische Universität, Darmstadt, Germany
[5]Gesellschaft für Schwerionenforschung Darmstadt, Darmstadt, Germany

(RECEIVED 18 June 2003; ACCEPTED 16 July 2003)

Abstract

Numerical analysis of the compression of a cylindrical cryogenic hydrogen sample surrounded by a high-density metallic shell driven by a heavy ion beam has been performed. The beam power profile is assumed to be parabolic in time and Gaussian in space and is made of uranium ions with a kinetic energy of 2.7 GeV/u. The beam center is positioned off axis and rotates around the target axis to provide a uniform annular energy deposition area. An acceptable symmetry in pressure is achieved if the number of revolutions is equal to or larger than 10. The maximum density and pressure of the hydrogen sample is studied as a function of the spread of the beam power Gaussian distribution and the rotation radius. This configuration leads to compressions of the order of 10 and a temperature of a few thousand Kelvin in hydrogen.

Keywords: Heavy ion beam; High density energy matter

1. INTRODUCTION

An intense heavy ion beam is a very promising driver to study equation-of-state (Zeldovich & Raizer, 1967) properties of matter under extreme conditions of density, pressure, and temperature (Stöwe *et al*., 1998; Hoffmann *et al*., 2000, 2002; Tahir *et al.*, 2000*a*, 2000*b*). Hydrogen is the most abundant element in the universe and its characteristics under extreme physical conditions are of great interest to planetary sciences, astrophysics (Anisimov *et al*., 1984), and inertial fusion (Lindl, 1995). Moreover it was predicted in 1935 (Wigner & Huntington, 1935) that when subjected to a pressure of 0.35 Mbar, the normal mono-atomic hydrogen, that is, an insulator, will transform into a metallic state (Nellis *et al.*, 1992; Weir *et al.*, 1996). Modern estimates, however, suggest that one may require a pressure of the order of a few megabar, a density of 1–2 g/cm^3, while the temperature should remain low (a few thousand Kelvin) in order to see this transition.

The heavy ion synchrotron SIS18 at the Gesellshaft für Schwerionenforschung (GSI) at Darmstadt will, in the future, provide high-intensity bunched pulses containing up to 2×10^{11} uranium ions with an ion energy of 200 MeV/u. Bunch lengths of a few hundred nanoseconds have already been achieved, and it is expected that, in the future, the bunch can be compressed to about 50 ns.

The currently available beam intensity is of the order of 10^{10} particle per bunch. GSI is also planning to build a new synchrotron facility, SIS100, that will deliver a much more intense uranium beam having up to 2×10^{12} ions per bunch. The ion kinetic energy will lie between 400 MeV/u and 3 GeV/u. The time compression of the bunch should provide a pulse length in the range of 90–20 ns.

The use of this intense heavy ion beam with an annular focal spot has been proposed to drive a cylindrical convergent shock wave allowing for compression of matter to high density and high pressure (Tahir *et al.*, 2001). However, creation of a beam with an annular focal spot is a challenging problem.

It has been recently suggested (Sharkov *et al*., 2001) that such an annular focal spot may be generated by a rotating beam. It is to be noted that the beam rotation would introduce an asymmetry in the energy deposition, thereby creating a nonuniform annular ring. We have carried out detailed analytic and numerical simulation work to determine the

Address correspondence and reprint requests to: M. Temporal, E.T.S.I. Industriales, Universidad de Castilla-La Mancha, 13071, Ciudad Real, Spain. E-mail: mauro.temporal@uclm.es

minimum rotation frequency that will be necessary to achieve an acceptable level of symmetry of the driving pressure (Piriz *et al.*, 2003*a*, 2003*b*). This study has shown that the asymmetry depends only on the number of the beam revolutions, N. Using a constant temporal pulse profile, the asymmetry $\propto 1/N$ (Piriz *et al.*, 2003*a*), whereas for a parabolic profile the asymmetry is $\propto 1/N^2$ (Piriz *et al.*, 2003*b*). Our study has shown that one would need about 10 revolutions of the rotating beam to achieve the required degree of asymmetry of the driving pressure (1%). In the analysis presented in the present article, we take into account a more realistic pulse that has a Gaussian spatial profile. Besides, because the beam profile now extends over the whole target, it also provides direct heating of the inner cylindrical sample as well.

The performance of the target compression has been studied by means of one-dimensional (1D) simulation using the code *MULTI*-1D (Ramis *et al.*, 1988). To analyze the nonuniformity of the target compression due to the rotation of the beam, we have performed two-dimensional (2D) simulations by using the *BIG2* code (Fortov *et al.*, 1996).

2. BEAM TARGET CONFIGURATION

A sketch of the considered beam-target configuration is shown in Figure 1. The target is a hollow cylinder of solid high-density material, for example, lead ($\rho_{\mathrm{Pb}} = 11.3\ \mathrm{g/cm^3}$) or gold ($\rho_{\mathrm{Au}} = 19.3\ \mathrm{g/cm^3}$). The sample material that has to be compressed is located inside the cylindrical cavity. We consider a cylindrical sample of cryogenic hydrogen at temperature $T_{\mathrm{H}} = 10$ K and density $\rho_{\mathrm{H}} = 0.0886\ \mathrm{g/cm^3}$. The radius of this cylinder is $R_{\mathrm{H}} = 400\ \mu$m.

As shown in Figure 1, the target length is smaller than the ion range (subrange target). The Bragg peak will therefore lie outside the target, which will lead to a fairly uniform energy deposition along the particle trajectory. We consider

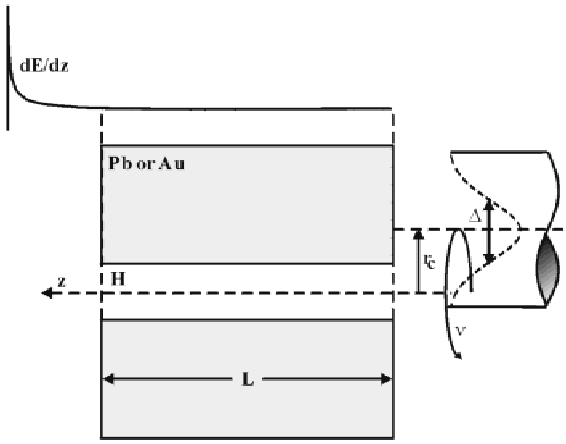

Fig. 1. Sketch of the beam–target configuration showing the rotating beam with a Gaussian power profile in space. The inner hydrogen cylinder is surrounded by a high-density absorber. The target length is shorter than the ion range.

that the target is driven by a heavy ion beam whose center is assumed to rotate with a frequency ν, forming a circular ring of radius r_c. The rotation frequency ν should be high enough to give a sufficiently uniform ion energy deposition to avoid a nonuniform cylindrical compression.

The heavy ion beam considered in the present study is formed by a bunch of uranium ions and is characterized by a parabolic intensity profile in time and a Gaussian shape in space. The total number of U ions in the bunch is assumed to be $N_{\mathrm{U}} = 2 \times 10^{11}$ and the ions are supposed to be accelerated up to a kinetic energy of 2.7 GeV/u.

The parabolic time dependence of the ion beam is given by

$$f(t) = \frac{6}{\tau^3}\,(t\tau - t^2), \tag{1}$$

where τ is the pulse duration. Presently, the SIS18 facility allows for a high compression of the ion bunch providing bunches of 300 ns duration. The future SIS100 facility at GSI is expected to be able to provide bunches with a temporal spread of a few tens of nanoseconds. In the present study, we consider a pulse length of $\tau = 100$ ns. The spatial ion beam profile has been considered to be Gaussian and is characterized by its full width at half maximum (Δ = FWHM).

The specific power deposition as a function of the radial coordinate r can be well approximated by the following equation:

$$P(r,t) = \frac{1}{\rho}\,\frac{dE}{dz}\,N_{\mathrm{U}}\,f(t)\,\frac{a e^{-a r_b(t)^2/\Delta^2}}{\pi\Delta^2} \tag{2}$$

where N_{U} is the number of uranium ions in the bunch and dE/dz is the ion stopping power, r_b is the instantaneous distance between the considered position r and the rotating beam center $\mathbf{r}_c(t)$. The distance r_b is a function of time given by $r_b^2 = r^2 + r_C^2 - 2 r_C r \cos(2\pi\nu t)$. Constant $a = -4\ln(1/2)$ is obtained by normalization to the total beam energy.

Due to the beam rotation, the energy deposition at a given angular position results in a series of $N = \nu\tau$ pulses that are modulated in time by the parabolic shape. In Figure 2, the profiles of the specific power deposition $P(r,t)$ as a function of time are shown. The lines correspond to the selected radii, $r = 0.0$, $r_c/3$, $2r_c/3$, and r_c, respectively. In this example, we consider a lead absorber and the beam parameters are $\nu = 100$ MHz, $\tau = 100$ ns, $dE/dz = 10^{10}$ [eV cm^2/g], and $N_{\mathrm{U}} = 2 \times 10^{11}$. These beam–target parameters allow for depositing of a total energy of 3.5 kJ/cm length in the target.

The specific energy deposition as a function of the radius r is evaluated by the time integral of Eq. (2). The numerical integration of $P(r,t)$ over the pulse duration τ provides the specific energy deposition, ε, shown in Figure 3. In this figure, the Gaussian shape of the ion beam pulse intensity is also shown (dotted line, arbitrary units). It is seen that due to the beam rotation, the maximum of the specific energy de-

https://doi.org/10.1017/S0263034603214208 Published online by Cambridge University Press

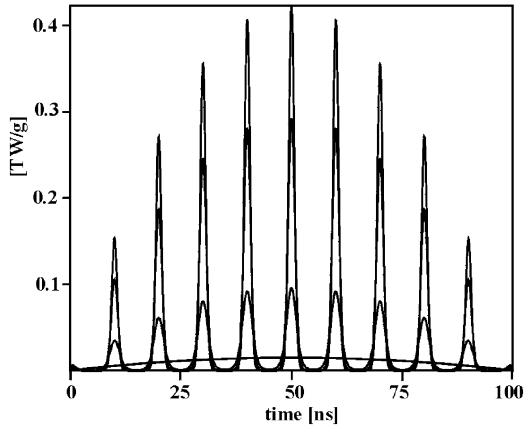

Fig. 2. Specific power deposition as a function of time evaluated at different radii; $r = 0.0$, $2r_c/3$, $r_c/3$, and r_c, where r_c is the radius of the trajectory of the center of the focal spot.

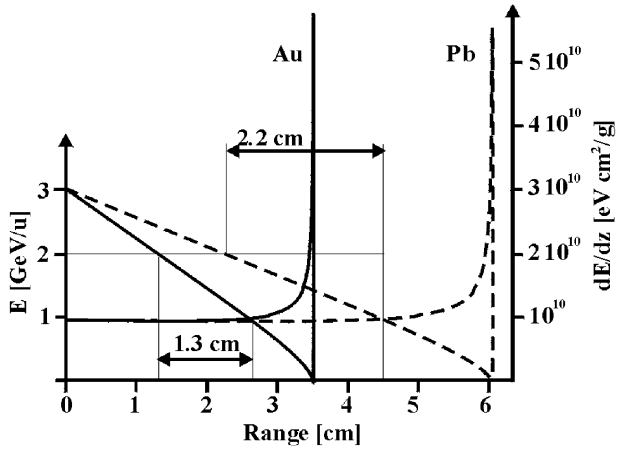

Fig. 4. Stopping power of U ions in Au (full line) and Pb (dotted line) solid targets versus the range. The residual ion kinetic energy is also shown.

position is shifted inward, and due to the long tail of the Gaussian distribution, the specific energy deposition is nonsymmetric and is higher at a lower radius. The total energy deposited per centimeter in the target as a function of the radius is also shown.

The stopping power of the uranium ions in a solid cold target has been calculated by using the code *SRIM* (Ziegler *et al.*, 1996). In Figure 4, the stopping power of a uranium ion in solid lead (dotted line) and in solid gold (solid line) has been plotted as a function of the range. In the same picture, the residual kinetic energy of the uranium ions have also been shown.

The calculations of these two stopping powers have been carried out considering that the initial kinetic energy of the U ions was 3 GeV/u. As is seen in Figure 4, the stopping power of the U ions with energy greater than 1 GeV/u is practically constant and is nearly equal to $dE/dz = 10^{10}$ eV cm^2/g in lead as well as in gold. By considering U ions accelerated to 2 GeV/u, the ion energy deposition results to be roughly constant over a distance bigger than $L_{\mathrm{Au}} = 1.3$ cm in gold and $L_{\mathrm{Pb}} = 2.2$ cm in lead. This allows one to use subrange targets with a relatively long length for which the specific energy deposition is practically uniform along the ion path. The *SRIM* code has also been used to evaluate the stopping power of the U ions passing through the cryogenic hydrogen. Of course, due to the very low density of the hydrogen, $\rho_{\mathrm{H}} = 0.0886$ g/cm^3, the range result is as large as 2.5 m. The value of the stopping power outside the Bragg peak zone is nearly constant at about $(dE/dz)_{\mathrm{H}} = 3.4 \times 10^{10}$ eV cm^2/g.

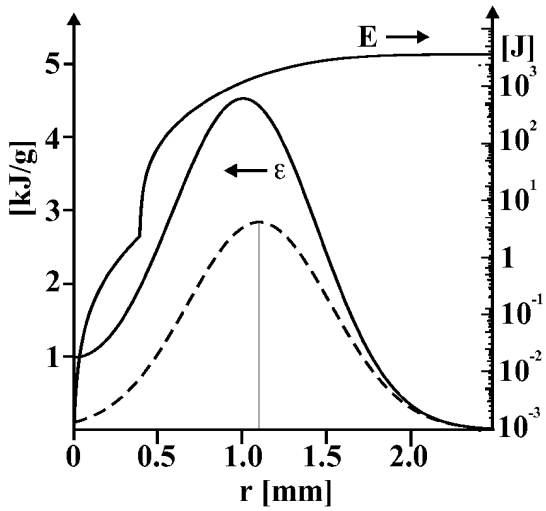

Fig. 3. Total time-integrated specific energy deposition, ε, and the integral of the total deposited energy, E, versus target radius. The intensity of the Gaussian beam profile is shown in arbitrary units (dotted line).

3. 1D TARGET COMPRESSION

A set of 1D simulations of the target dynamics has been performed using the *MULTI*-1D code. The beam parameters were considered to be those available at the future SIS100 facility at the GSI Darmstadt.

A set of simulations has been performed by considering a total number of 2×10^{11} ions per bunch and a Gaussian pulse shape with $\Delta = 1$ mm and pulse length $\tau = 100$ ns. For these cases, the absorber is considered to be made of lead. For each simulation, we looked for the maximum density and temperature of the central hydrogen sample. The radial position of the rotating beam center, r_c, is increased starting with the case of coaxial focal spot, $r_c = 0$ up to 3.5 mm. The results are shown in Figure 5, where the full line corresponds to the average maximum hydrogen density (g/cm^3) and the dotted line corresponds to the maximum hydrogen temperatures in electron volts.

These results clearly show that there are two regions: one corresponding to relatively smaller radii r_c providing lower hydrogen compression and the second, for large radii r_c, that allows for higher target compression. If the rotating beam

https://doi.org/10.1017/S0263034603214208 Published online by Cambridge University Press

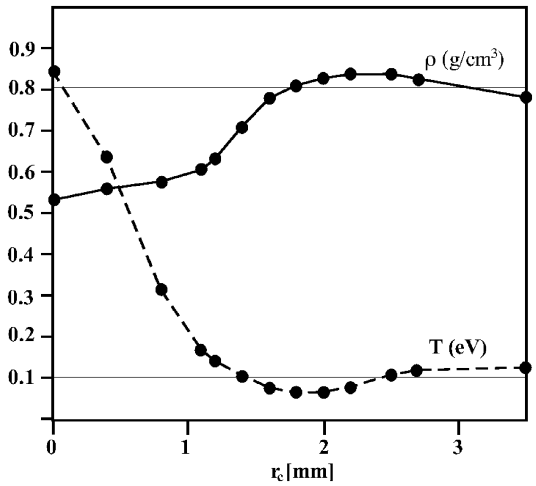

Fig. 5. Average hydrogen density (full line) and temperature (dotted line) achieved at stagnation, as a function of the radius r_c. The data refer to the target with a Pb absorber and a Gaussian beam with $\Delta = 1$ mm.

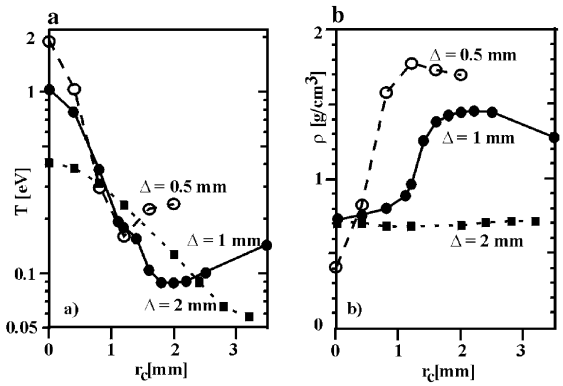

Fig. 6. Average maximum hydrogen temperatures (a) and density (b) as a function of radius r_c for beams with different values of the FWHM: $\Delta = 0.5$ (void circle), 1 (full circle), and 2 mm (box). The data refer to a target made of an Au absorber.

center is situated at around 1.8 mm, the temperature is lower than 0.1 eV and the hydrogen density becomes higher than 0.8 g/cm^3. This stepped behavior can be qualitatively understood by considering that only a relatively large value of the beam center, r_c, allows for the generation of a shaped energy deposition. This shaping creates a zone within the absorber just outside the hydrogen sample that is characterized by a lower specific energy deposition. This zone acts as an inertial pusher that leads to more efficient dynamics of the compression. At the same time a larger r_c reduces the energy deposited in the inner hydrogen sample, allowing for a higher compression.

Analogous simulations have been performed considering a gold absorber instead of lead. A set of simulation has also been done varying the FWHM of the Gaussian distribution. Namely, we consider $\Delta = 0.5$, 1, and 2 mm. In these simulations we still use the same beam intensity $N_U = 2 \times 10^{11}$. The results concerning the maximum average hydrogen temperature and maximum density are shown in Figures 6a and 6b, respectively.

As seen clearly in Figure 6b, corresponding to the Gaussian pulse with a $\Delta = 1$ mm, the density increases in comparison with the previous case when a lead absorber has been used. With the gold absorber, the maximum average hydrogen density increases up to 1.4 g/cm^3. It is also to be noted that using a Gaussian shape with a smaller spread (see the cases with $\Delta = 0.5$ mm), the maximum density increases up to 1.8 g/cm^3 for a radius $r_c = 1.2$ mm. In contrast, by considering a wider Gaussian profile with a $\Delta = 2$ mm, the density is reduced and is nearly constant, close to $\rho = 0.7$ g/cm^3. This is because the beam heats a larger absorber mass, thus reducing the specific deposited energy. Moreover, the long Gaussian tail avoids the generation of an efficient pusher, contributing also to the preheating of the central hydrogen sample. Both effects play a negative role, thereby avoiding an efficient hydrogen compression.

Figure 7 shows the time evolution of the interface between the absorber and the hydrogen and the average density of the hydrogen. The results correspond to the case of a gold absorber using a Gaussian beam profile with $\Delta = 1$ mm and $r_c = 1.8$ mm. The parabolic time dependence of the beam is plotted in the same figure. It is seen that during the first 100 ns, when the beam is still switched on, there is practically no motion of the absorber–hydrogen interface. A few hundred nanoseconds after the end of the pulse, the shock reaches the hydrogen sample and its compression is initiated. Stagnation is reached at around 500 ns, and a maximum density larger than 1.4 g/cm^3 is achieved providing a compression factor of around 16.

It is interesting to note that, considering a wider Gaussian distribution, the final hydrogen density result is practically constant, as shown in Figure 6. The final hydrogen compression is quite large even in the case when the beam is just

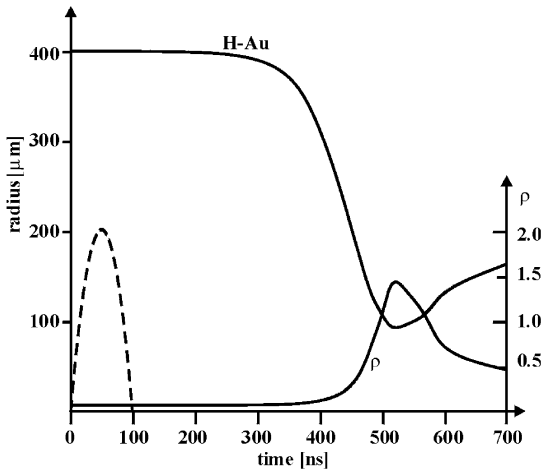

Fig. 7. Temporal evolution of the hydrogen–gold interface and of the average hydrogen density. The parabolic beam power profile is shown in arbitrary units (dotted line).

https://doi.org/10.1017/S0263034603214208 Published online by Cambridge University Press

centered and aligned with the cylindrical sample ($r_c = 0$) and it is not rotating. In this case, the temperature is higher than in the previous case, about 0.4 eV. However, a study of the EOS of hydrogen in this region is also of great scientific interest.

A series of simulations for different values of Δ using the same conditions as before has also been done. The maximum hydrogen compression and sample temperature are shown in Figure 8 as a function of the FWHM beam spread. The hydrogen density and temperature slowly decrease as the FWHM increases. Although the temperature decreases rapidly, for a large Gaussian spread (see, e.g., the data at Δ = 3 mm), it is reduced to 0.24 eV.

The relatively high temperature of the sample arises from the fact that it is directly heated by the uranium ions. An ideal solution to provide high density at a lower temperature is to consider a high-density cylindrical plug between the incoming ions and the hydrogen sample. This mask must have the same radius as the central sample, thus avoiding the direct heating of the inner hydrogen. In the same figure we have also reported the densities and temperatures (dotted lines) reached neglecting the energy deposition of the ions entering into the hydrogen.

As expected, in this case, the hydrogen is compressed more efficiently (e.g., Δ = 2 mm allows for $\rho > 1$ g/cm^3) and at the same time the temperature is reduced below the level of 1000 K.

4. ANALYSIS OF THE NONUNIFORMITY

The study of the nonuniformity generated by a rotating beam (peak-to-valley of the target surface) has been recently presented. It has been pointed out that the asymmetry depends on the time profile of the pulse and on the number of beam revolutions N (Piriz *et al.*, 2003*a*). For a parabolic time profile, we have found that the relative asymmetry $\Delta p/p$ (Piriz *et al.*, 2003*b*) in the driving pressure is proportional to $1/N^2$ (p is the mean pressure in the absorber layer at the end of the pulse).

In the present case, we have performed a series of simulations with a version of a 2D hydro-code *BIG2* that include the energy deposition due to the rotating beam. In such simulations, we have used a Gaussian energy distribution for the beam focal spot with a parabolic temporal power profile. Besides, we have considered the optimal case corresponding to $r_c = 1.8$ mm. In Figure 9, we present the simulation results showing that the pressure asymmetry $\Delta p/p$ is still proportional to $1/N^2$.

An asymmetry of the level of 1% can be achieved by considering a rotating beam system able to generate a minimum number of beam revolutions, $N_{1\%}$, during the beam pulse. As is shown in Figure 9, such a threshold lies around $N_{1\%} = 10$ for the Gaussian profile, similar to the results obtained previously for a parabolic energy distribution (Piriz *et al.*, 2003*b*).

5. CONCLUSIONS

A parametric analysis of the maximum compression of a hydrogen sample has been presented. The compression is achieved by means of implosion of a multilayered cylindrical target driven by a rotating heavy ion beam.

Two-dimensional simulations of the azimuthal asymmetry have been performed considering a parabolic beam power profile in time and a Gaussian profile in space. The results confirm the dependence of the asymmetry on the number of beam revolutions that is proportional to $1/N^2$, the same as obtained in a previous study using a parabolic profile in space.

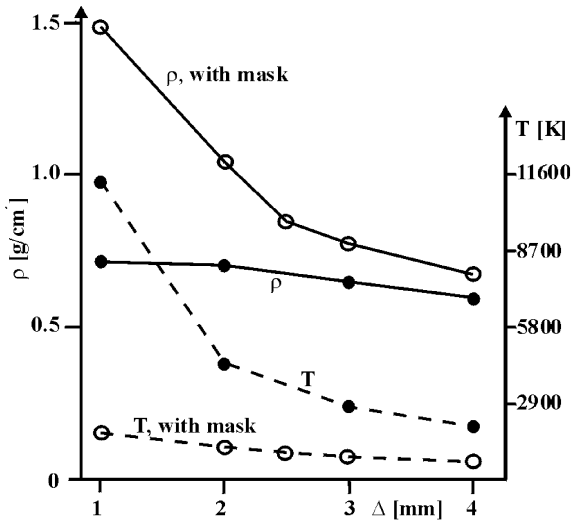

Fig. 8. Hydrogen density and temperature at the stagnation versus Δ. Full circles correspond to the case where the ion beam is axially aligned with the target ($r_c = 0.0$). See the main text for the meaning of the data labeled *with mask* (void circles).

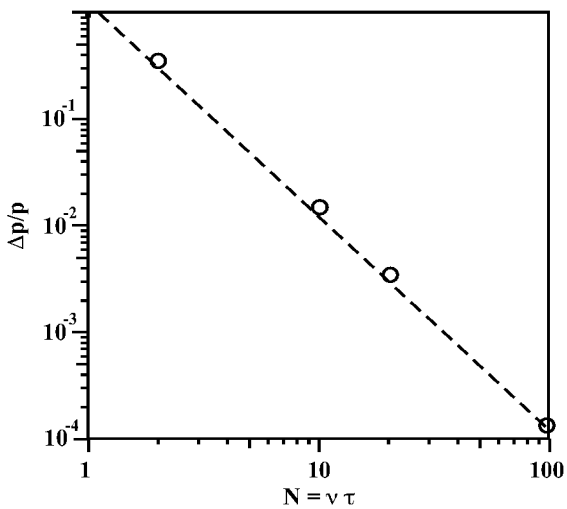

Fig. 9. Relative pressure asymmetry $\Delta p/p$ versus the beam revolutions number, N, where p is the mean pressure in the absorber layer at the end of the pulse.

https://doi.org/10.1017/S0263034603214208 Published online by Cambridge University Press

One-dimensional simulations have been performed considering two materials, gold and lead, for the target absorber. It has been found that a more efficient hydrogen compression can be achieved by using a gold absorber instead of lead. Hydrogen compressions as high as 1.4 g/cm^3 at temperatures lower than 0.1 eV have been reached by considering a uranium ion bunch length of $\tau = 100$ ns consisting of 2×10^{11} ions, which is characterized by a Gaussian spatial profile with a FWHM = 1 mm and rotating along a circle with a radius of around $r_c = 1.8$ mm. Relevant high-density, low-temperature hydrogen states have also been obtained by considering a nonrotating beam axially aligned. In this case, the central hydrogen cylindrical sample must to be masked by a high-density plug to avoid direct hydrogen heating. This latter configuration requires further studies to understand the hydrodynamics of the ion-stopping mask.

ACKNOWLEDGMENTS

M.T., A.R.P., and N.G. thank the staff of the Heavy Ion Plasma Physics Group at the GSI Darmstadt for their hospitality during the stay at GSI. This work has been financially supported by the BMBF (Germany) and the Consejeria de Ciencia y Tecnologia-JCCM-PAI-02-002 (Spain).

REFERENCES

Anisimov, S.I., Prokhorov, A.M. & Fortov, V.E. (1984). Application of powerful laser in dynamical physics of high pressure. *Sov. Phys. Usp*. **27**, 181–220.

Fortov, V.E., Goel, B., Munz, C.D., Ni, A.L., Shutov, A.V. & Vorobiev, O.Yu. (1996). Numerical simulations of nonstationary fronts and interfaces by Godunov method in moving grids. *Nucl. Sci. Eng*. **123**, 169–189.

Hoffmann, D.H.H., Bock, R., Faenov, Ya.A. Funk, U., Geissel, M., Neuner, U., Pikuz, T.A., Rosmej, F., Roth, M., Süss, W., Tahir, N.A. & Tauschwitz, A. (2000). Plasma physics with intense laser and ion beams. *Nucl. Instrum. Methods Phys. Res. B* **161**, 9–18.

Hoffmann, D.H.H., Fortov, V.E., Lomonosov, I.V., Mintsev, V., Tahir, N.A., Varentsov, D. & Wieser, J. (2002). Unique capabilities of an intense heavy ion beam as a tool for equation-of-state studies. *Phys. Plasmas* **9**, 3651–3654.

Lindl, J. (1995). Development of the indirect-drive approach to inertial confinement fusion and the target physics basis for ignition and gain. *Phys. Plasmas* **2**, 3933–4024.

Nellis, W.J., Mitchell, A.C., McCandless, P.C., Erskine, D.J. & Weir, S.T. (1992). Electronic energy gap of molecular hydrogen from electrical conductivity measurements at high shock pressures. *Phys. Rev. Lett*. **68**, 2937–2940.

Piriz, A.R., Tahir, N.A., Hoffmann, D.H.H. & Temporal, M. (2003*a*). Generation of a hollow ion beam: Calculation of the rotation frequency required to accommodate symmetry constraint. *Phys. Rev E* **67**, 017501-1-3.

Piriz, A.R., Temporal, M., Lopez Cela, J.J., Tahir, N.A., Hoffmann, D.H.H. (2003*b*). Symmetry analysis of cylindrical implosions driven by high frequency rotating ion beams. *Plasma Phys. Controlled Fusion* **45**, 1733–1745.

Ramis, R., Schmalz, R. & Meyer-ter-Vehn, J. (1988). MULTI—A computer code for one-dimensional multigroup radiation hydrodynamics. *Comp. Phys. Com*. **49**, 475–505.

Sharkov, B.Yu., Alexeev, N.N., Churazov, M.D., Golubev, A.A., Koshkarev D.G. & Zenkevich, P.R. (2001). Heavy ion fusion energy program in Russia. *Nucl. Instrum. Methods A* **464**, 1–5.

Stöwe, S., Bock, R., Dornik, M., Spiller, P., Stetter, M., Fortov, V.E., Mintsev, V., Kulish, M., Shutov, A., Yakushev, V., Sharkov, B., Golubev, S., Bruynetkin, B., Funk, U., Geissel, M., Hoffmann, D.H.H. & Tahir, N.A. (1998). High density plasma physics with heavy-ion beams. *Nucl. Instrum. Methods Phys. Res. A* **415**, 61–67.

Tahir, N.A., Hoffmann, D.H.H., Kozyreva, A., Shutov, A., Maruhn, J.A., Neuner, U., Tauschwitz, A., Spiller, P. & Bock, R. (2000*a*). Shock compression of condensed matter using intense beams of energetic heavy ions. *Phys. Rev. E* **61**, 1975–1980.

Tahir, N.A., Hoffmann, D.H.H., Kozyreva, A., Shutov, A., Maruhn, J.A., Neuner, U., Tauschwitz, A., Spiller, P. & Bock, R. (2000*b*). Equation-of-state properties of high-energy-density matter using intense heavy ion beams with an annular focal spot. *Phys. Rev E* **62**, 1224–1233.

Tahir, N.A., Hoffmann, D.H.H., Kozyreva, A., Tauschwitz, A., Shutov, A., Maruhn, J.A., Spiller, P., Neuner, U., Jacoby, J., Roth, M., Bock, R., Juranek, H. & Redmer, R. (2001). Metallization of hydrogen using heavy-ion-beam implosion of multilayered cylindrical targets. *Phys. Rev. E* **62**, 016402-1-9.

Weir, S.T., Mitchell, A.C. & Nellis, W.J. (1996). Metallization of fluid molecular hydrogen at 140 GPa (1.4 Mbar). *Phys. Rev. Lett*. **76**, 1860–1863.

Wigner, E. & Huntington, H.B. (1935). The possibility of a metallic modification of hydrogen. *J. Chem. Phys*. **3**, 764–770.

Zeldovich, Y.B. & Raizer, Y.P. (1967). *Physics of Shock Wave and High Temperature Hydrodynamic Phenomena*. New York: Academic Press.

Ziegler, J.F., Biersack, J.P. & Littmark, U. (1996). *The Stopping and Ranges of Ions in Solids*. New York: Pergamon.